Kresling Origami-Based, Magnetically Actuated Crawling Robot for Drug Delivery

Undergraduate Honors Research Thesis

Completed in Partial Fulfillment of the Requirements for Graduation with Honors Research Distinction in the Department of Mechanical Engineering at The Ohio State University

Jun Nishikawa

April 2021

Thesis Defense Committee:

Ruike Zhao, Ph.D., Advisor

Jonathan Song, Ph.D.

Abstract

Origami has recently been applied in fields such as metamaterials, aerospace engineering, and biomedical engineering. All these applications take advantage of origami structures' ability to deploy and change shapes easily while being lightweight and compact. In the field of biomedicine, small origami structures have been researched for applications like disease diagnosis, drug delivery, and minimally invasive surgery. However, these soft origami machines face difficulties when navigating through highly confined or viscous areas in the body. The Kresling origami pattern can be useful in addressing this issue as it has several important properties ideal for functioning inside of the body. Namely, it has an anisotropic stiffness characteristic that allows it to withstand lateral resistance while still deforming in the axial direction, and it naturally has an internal space where medical supply could be stored safely. The goal of this research was to construct and characterize a Kresling origami-based crawling robot that is untethered and compact. The robot has magnetically responsive materials installed on it and is controlled via electromagnets. Magnetic actuation separates the power source and controller from the actuator, which untethers the robot and reduces the number of constituent parts. By manipulating the applied magnetic field strength and direction, the robot can be controlled as desired. The resulting Kresling origami robot in this research can fit within a 1 cm by 1 cm by 3 cm volume, weighs about 1 gram, and can be controlled freely in the horizontal plane by applying magnetic fields of up to 40 mT in strength. It can crawl within a confined space comprised of mimicked human tissue layers. Additionally, it has been demonstrated to successfully store and release a water-soluble dye which simulates drug delivery. Characterization of the robot involved determining how parameters of the magnetic field profile affects performance such as the speed and stride length.

Table of Contents

List of Figures

Introduction

Background

Origami, the Japanese art of paper folding, is widely recognized for its aesthetic qualities. Recently, origami has been used for more practical applications in fields such as metamaterials [1], aerospace engineering [2], and biomedical engineering [3]. All these applications take advantage of origami structures' ability to deploy and change shapes easily.

In the field of biomedicine, centimeter- to millimeter-scale origami structures have been researched for applications like disease diagnosis [4], drug delivery [5], and minimally invasive surgical procedures [6]. Their small size allows them to be introduced into the human body easily and access specific locations. However, these origami machines face difficulties when navigating through highly confined or viscous areas in the body. Many of them use soft materials, which are incapable of overcoming large resistances.

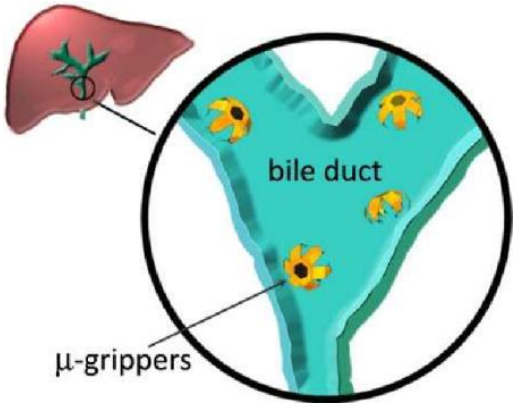

Figure 1: An origami-inspired gripper robot for biopsy [4]

The Kresling origami pattern shown below in Figure 2 is particularly useful in addressing this issue. It is a column-like, prismatic structure that can be deployed and folded by either applying a force in the axial direction or applying a torque to the ends. The structure undergoes coupled longitudinal and rotational motions as it transitions between those two states. Because of its shell structure, the Kresling origami naturally has an internal cavity which can store things like drugs. Furthermore, this structure has anisotropic stiffnesses in the axial and lateral directions, allowing it to withstand lateral direction stresses while still being mobile in the axial direction.

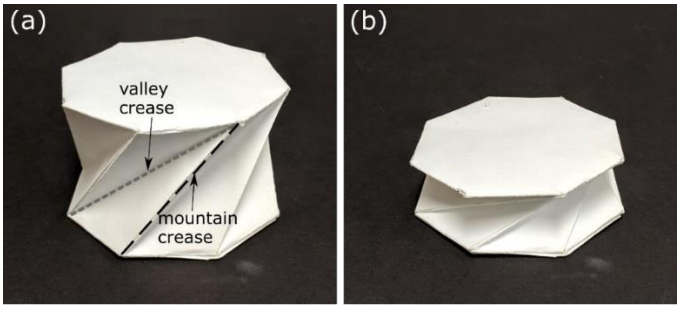

Figure 2: Kresling origami in deployed (left) and folded (right) states [7]

By attaching a magnetic disk to the hexagonal ends of the Kresling origami, it can be deployed and folded via an external magnetic field [8]. The magnetic disk rotates to align its magnetization orientation with the applied magnetic field, which generates torque and twists the origami structure. Since the external device generating the magnetic field is not physically connected to the Kresling origami structure, this method allows untethered actuation. The whole structure can be easily downscaled since it does not need an on-board power source or controller.

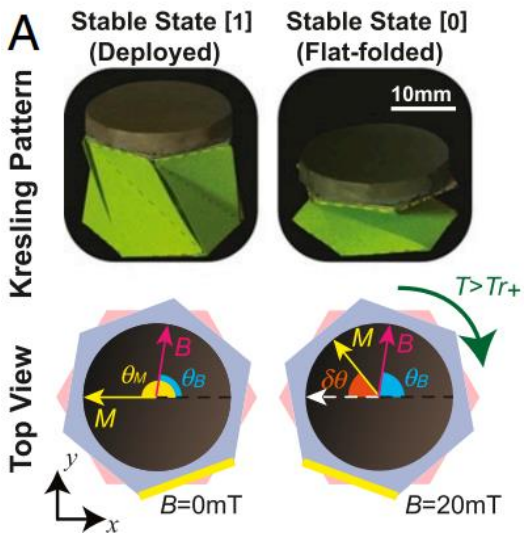

Figure 3: Magnetic actuation of Kresling origami [8]

Research Goal

The primary goal of this research was to develop a small-scale crawling robot that can potentially navigate within the human body and perform targeted drug delivery. This was based on the hypothesis that a robot built from magnetically actuated Kresling origami cells can effectively traverse confined spaces while carrying a load of drug. Magnetic actuation separates the power source and controller from the actuator, untethering the robot and allowing it to be downscaled easily. By manipulating the magnetic field strength and direction applied, the robot can be controlled as desired.

Another goal was to demonstrate and characterize the performance of the crawling robot. Specific motions and tasks were recorded to demonstrate how controllable the robot is via magnetic actuation. Also, quantitative data on the relationship between the applied magnetic field characteristics and the motion of the robot were studied. The results from this research will hopefully pave the way towards further development of the crawling robot and clinical tests to validate its performance in the human body.

Significance

Small-scale, soft robots that are capable of navigating within the human body have many potential applications for medical procedures. Though this paper only discusses targeted drug delivery, tasks like disease diagnosis and surgery can also be performed through further development of these robots. Because the robots are small, they can be easily introduced into the body through orifices (mouth, anus, etc.) or through small incisions, thus making the procedure minimally invasive. Compared to traditional methods, minimally invasive procedures result in less pain, less risks of infection, and faster recovery for patients.

Materials & Methods

Robot Structure & Mechanism

The crawling Kresling robot consists of three main components: the Kresling unit cells, soft magnetic discs, and feet, as labeled in Figure 4 below. For a sense of scale, the robot has a length of 28 mm and a mass of about 1 gram.

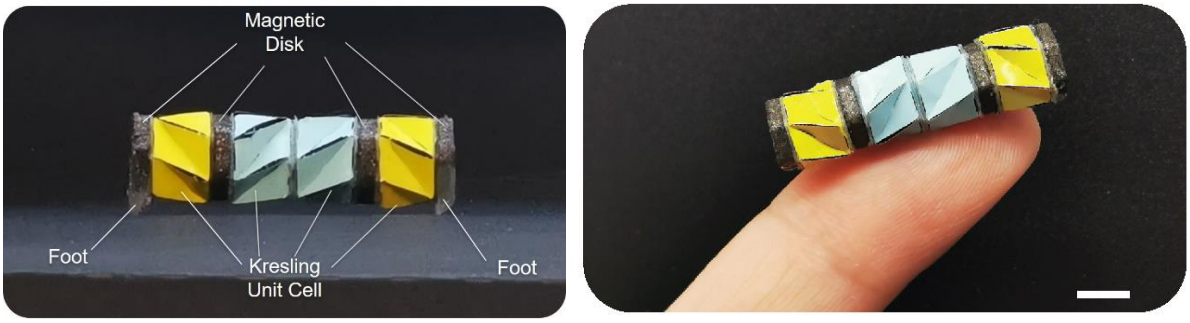

Figure 4: Kresling crawling robot with parts labeled (left), robot on finger for scale (right)

Four Kresling unit cells made of 0.05 mm polyethylene film are used per robot. Polyethylene's water resistance is ideal for using the robot in aqueous environments, and the particular thickness of the sheet provides an appropriate amount of stiffness to be magnetically actuated. The middle two cells (in blue) have creases in the clockwise direction, while the outer two cells (in yellow) have creases in the counterclockwise direction as shown in Figure 5. The two types are essentially mirror images of each other in structure.

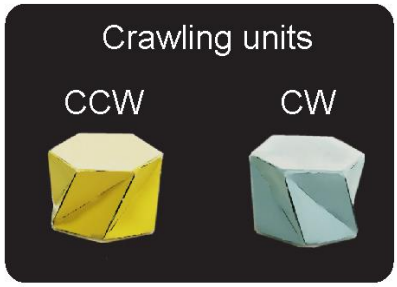

Figure 5: Two types of Kresling unit cells used on robot

Four soft magnetic disks, made from a mixture of Ecoflex-0030 silicone and neodymium-iron-boron (NeFeB) microparticles, are used per robot. The two material are mixed at 40 volume percent and poured into hexagonal molds with an edge length *s* of 3.9 mm and thickness of 1.4mm as shown in Figure 6. The molds are 3D printed with an Ultimaker S5 Printer and the material is polylactic acid (PLA). For the disks with a through-hole in the center, the hole diameter *d* is 2.5 mm. The disks are cured at 80 °C for approximately 30 minutes in an oven. Once completely cured, each disk is magnetized with a 1.5 T impulse magnetic field in the orientations shown in Figure 6.

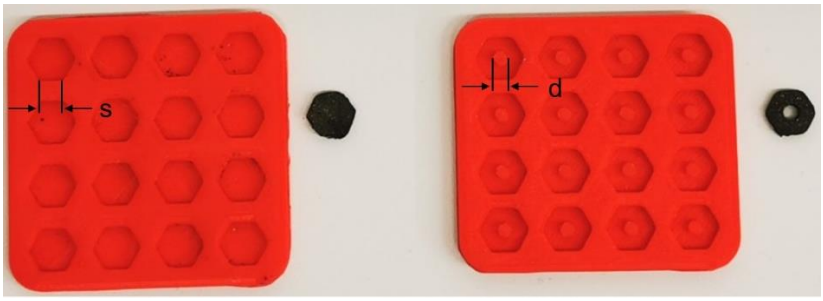

Figure 6: 3D printed PLA molds and magnetic disks

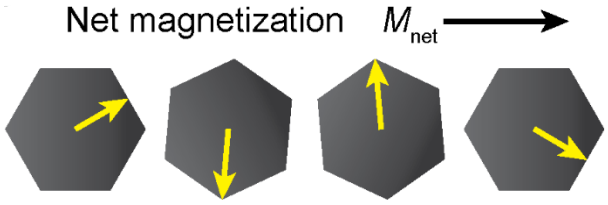

Figure 7: Magnetization orientations of magnetic disks and net magnetization of all four

The robot has two feet that are attached to the magnetic disks on the end as seen in Figure 8. Their anisotropic friction characteristic allows the robot to slide forward during the contraction and expansion phases. The base is molded from polydimethylsiloxane (PDMS) with a base to curing agent ratio of 5:1, which has a relatively high coefficient of friction. A strip of acetate tape is attached to the angled face of the PDMS feet, which has a relatively low coefficient of friction.

As shown in Figure 9, the high friction portion of the front foot and the low friction portion of the back feet contact the ground during the contraction phase. During the expansion phase, the high friction portion of the back foot and the low friction portion of the front foot contact the ground. The net distance the robot travels after one cycle of contraction and expansion is its

stride length. Figure 10 illustrates an example of the profile of the magnetic field applied during both phases. The field strength ramps up from 0 to 40 mT during the contraction phase, reaches peak contraction at 40 mT, and ramps back down to 0 mT during the expansion phase. The length of time taken to complete the cycle is the period, ***T***, which is 0.6 s in this case.

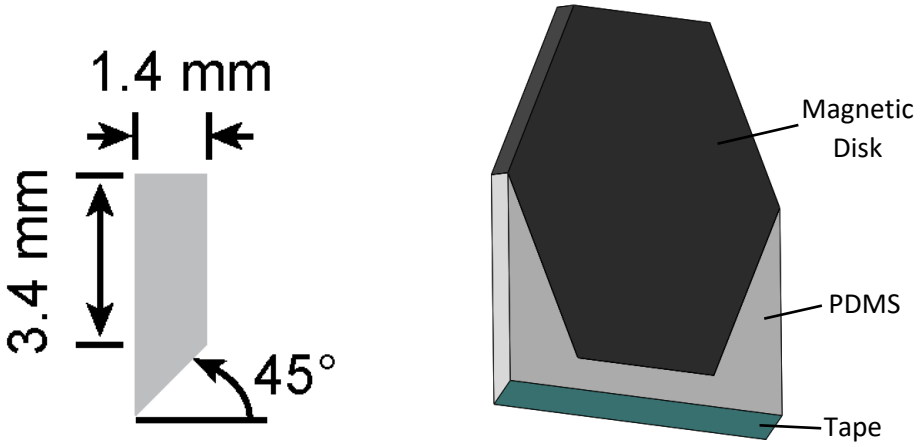

Figure 8: Dimensions of PDMS feet (left), assembly of feet and mangetic disk (right)

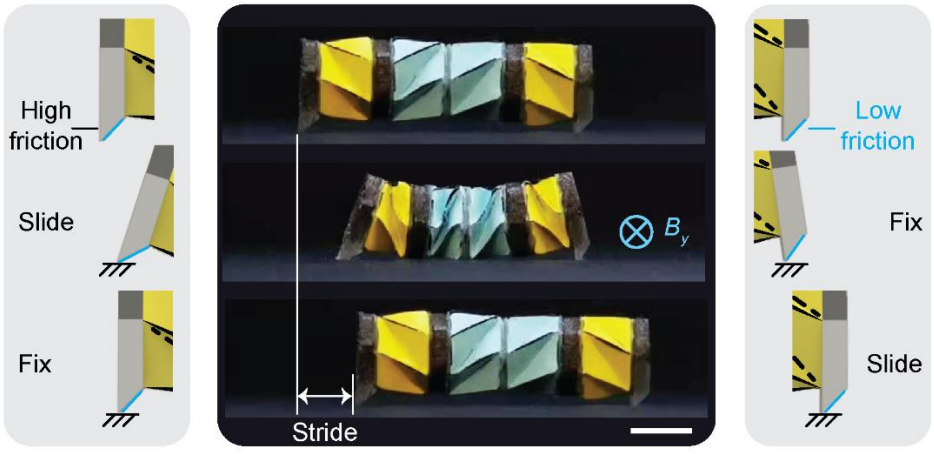

Figure 9: Mechanism for crawling

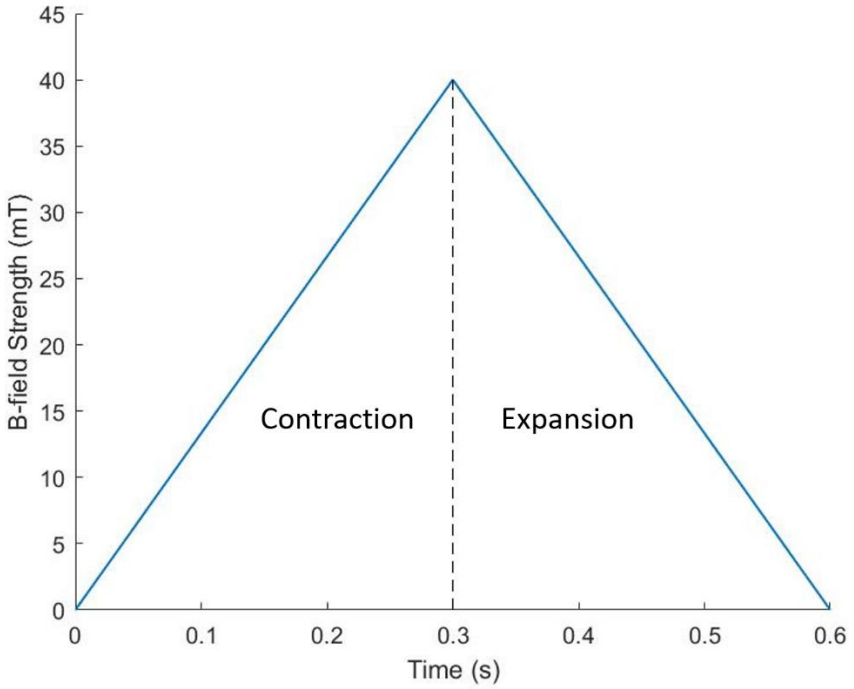

Figure 10: Example of magnetic field profile showing contraction and expansion phases

Testing and Characterization

A custom 3D Helmholtz coil, shown in Figure 11, is used to produce the magnetic field necessary to actuate the crawling robot. It is comprised of three sets of electromagnetic coils with their axes orthogonal to each other such that they generate magnetic fields in the X, Y, and Z directions. Each set of coils can produce up to 40 mT in magnetic field strength due to hardware limitations. The direction, amplitude, and timing of the field can be controlled through a custom MATLAB script.

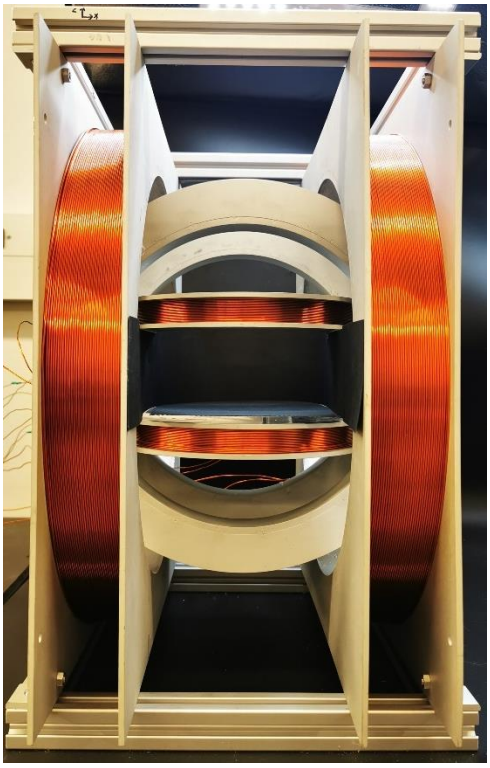

Figure 11: Three-dimensional Helmholtz coils for generating magnetic fields

All demonstrations and tests except for the crawling in a confined space are performed with the robot on top of black construction paper. The crawling in a confined space is done on a substrate of polydimethylsiloxane (PDMS), which is detailed in the *Crawling Within Confined Space* section.

Results

2D Motion

By using the three-axis Helmholtz coil, the crawling robot can be controlled freely in the 2D plane. In this paper, the *XYZ* directions define the global coordinate system and the *xyz* directions define the local coordinate system on the robot itself.

As Figure 7 showed in the previous chapter, the four magnetic disks have a net magnetization of $\mathbf{M}_{\mathbf{net}}$. This is always along the *y* direction of the robot, and the entire robot will rotate when a magnetic field is applied such that $\mathbf{M}_{\mathbf{net}}$ aligns with the magnetic field direction. Figure 12 shows a demonstration in which 10 mT impulse magnetic fields are applied at 60° intervals which causes the robot to also rotate at 60° intervals. Note that a 10 mT impulse is insufficient to cause an appreciable contraction of the robot and can only cause rotation.

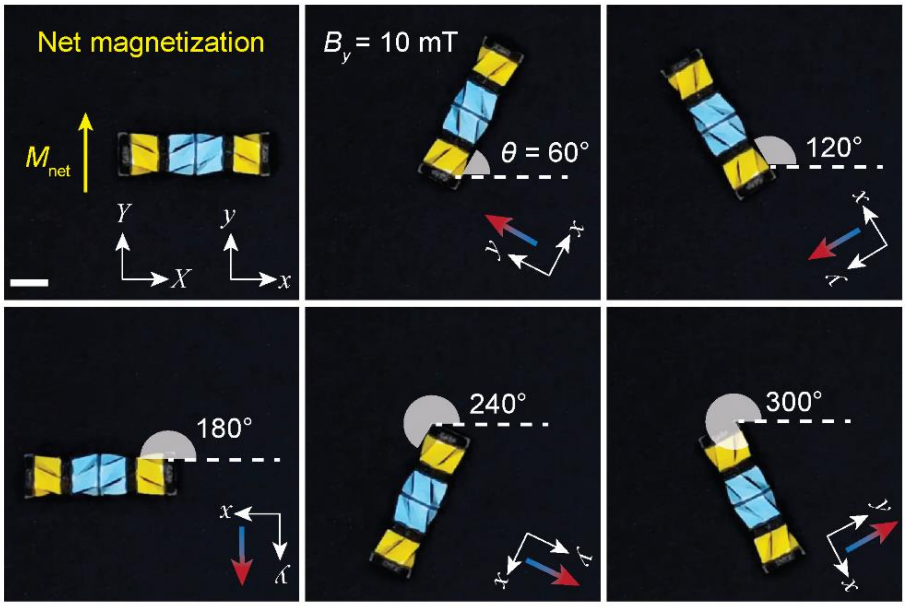

Figure 12: Robot rotating in 60° increments in the XY plane

By combining the robot's ability to crawl forward and its ability to rotate, it can be controlled to freely traverse the *XY* plane. Figure 13 shows two demonstrations in which the robot crawls in a predetermined Z-shaped path and an O-shaped path. The Z-shaped path consists of three straight segments: the robot first moves forward in the *X* direction, rotates -130° with respect to the *X*-axis, moves forward, rotates 130°, then moves forward in the *X* direction again. The O-shaped path is traveled by continuously changing the robot's angle from 0° to 360° while crawling forward. Magnetic fields of a maximum strength of 30 mT and a period of 0.6 s were used for both demonstrations.

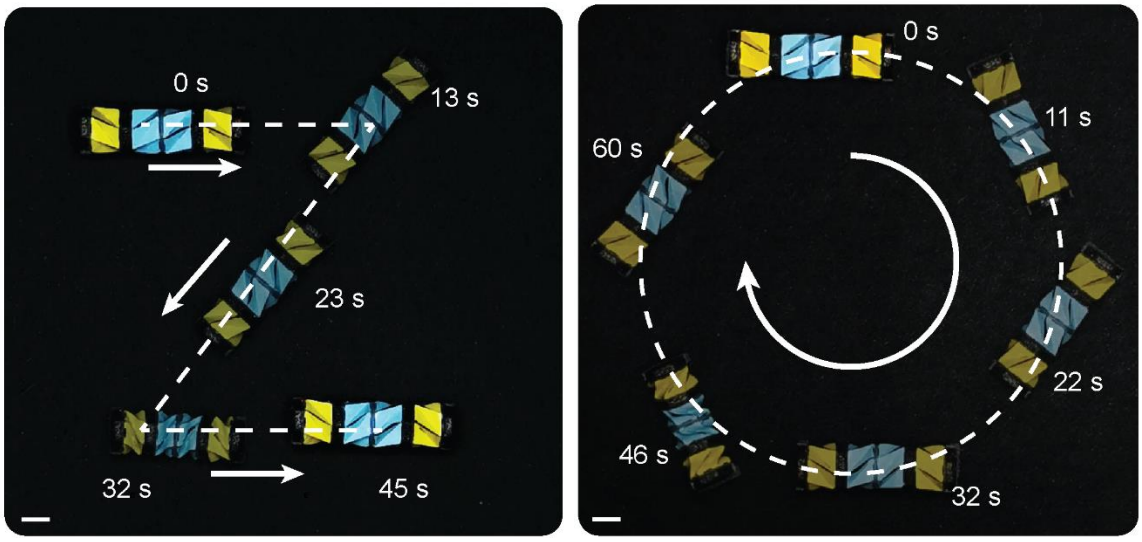

Figure 13: Robot crawling in Z-shaped path (left) and O-shaped path (right)

Contraction vs Magnetic Field Strength

The Kresling robot is in the expanded state by default and contracts under an applied magnetic field. It is therefore important to know how strong of a magnetic field must be applied to drive the crawling motion effectively. Figure 14 illustrates the relationship between the amount of

contraction, given as a percent of the robot's original length, versus the magnetic field strength. The contraction is given by the following equation, where ***L*** and ***l*** are defined in Figure 15:

$$Contraction\ (\%) = \frac{L - l}{L} * 100$$

The amount of contraction generally increases as the strength of the magnetic field increases. The increase is non-linear, however, due to the stress-compression characteristic of each Kresling unit cell and the magnetic force interactions occurring between the magnetic plates as they approach one another.

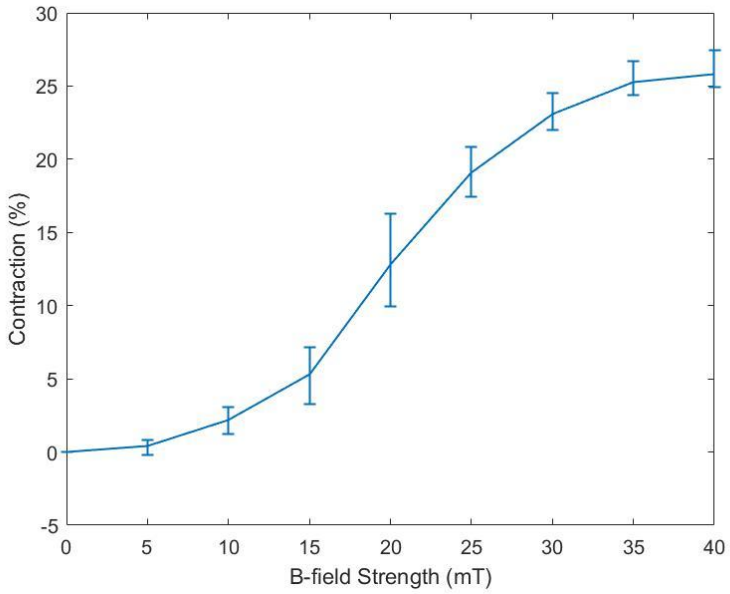

Figure 14: Contraction as percent of original length vs magnetic field strength

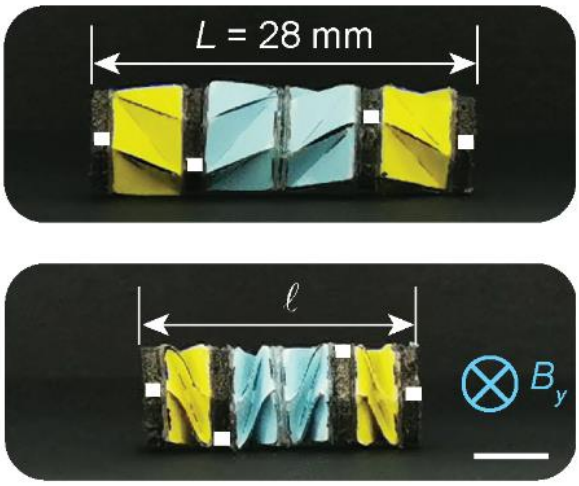

Figure 15: Robot in expanded state and contracted state

Stride vs Period vs Magnetic Field Strength

The stride as a function of magnetic field strength and period is shown in Figure 16. The stride of the robot is defined as the linear distance it travels after one full cycle of contraction and expansion. The period ***T*** is the amount of time taken to complete one full cycle of contraction and expansion. As the magnetic field strength increases, the stride also increases. This makes sense since the amount of contraction increases as the magnetic field strength increases, as seen in Figure 13 from the previous section. A magnetic field cycle period of 0.4 s generally results in the most optimal displacement per cycle while a period of 0.2 s results in the worst. At low periods, the contraction and expansion occur quickly, and the feet could be seen slipping on the surface often. This results in less efficient motion for the robot and thus leads to smaller strides. Note that a field of 10 mT or less does not result in any appreciable stride since the amount of contraction is too small to overcome the friction of the feet.

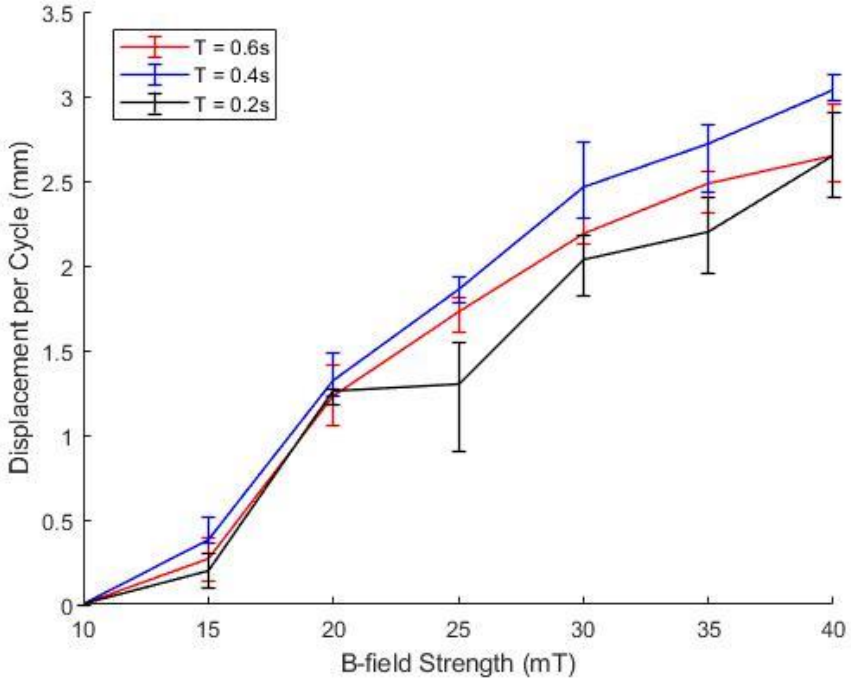

Figure 16: Effect of magnetic field strength and cycle period on displacement per cycle

Speed vs Period vs Magnetic Field Strength

The speed of the crawling robot is similarly affected by both the cycle period and the amplitude of magnetic field strength. Interestingly, although a period of 0.2 s results in more slipping and less efficient motion, the average speed is the highest. However, the variability in speed was also the highest. A period of 0.6 s resulted in the slowest motion.

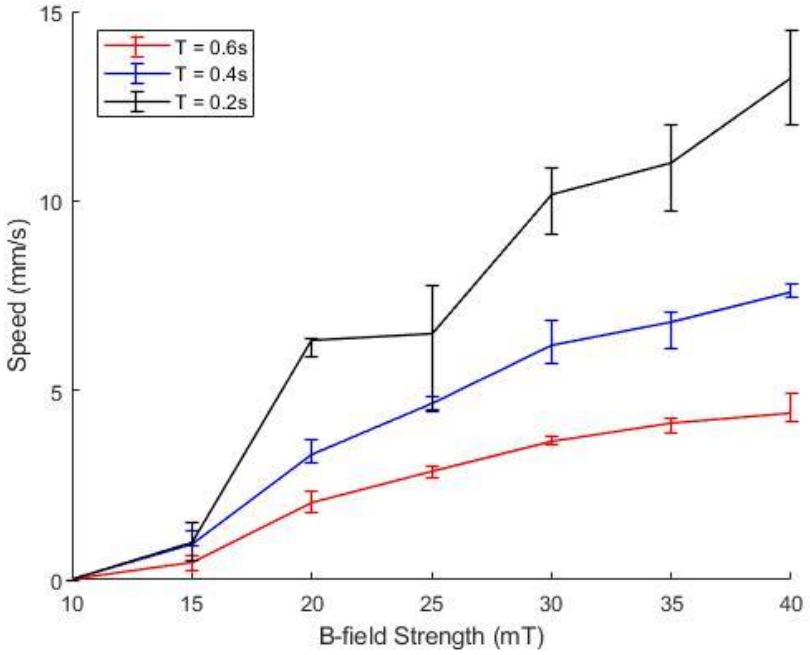

Figure 17: Effect of magnetic field strength and cycle period on speed

Crawling Within Confined Space

Figure 18 demonstrates the robot crawling through a confined space that mimics a possible environment within the human body. The substrate on the bottom and the film on top are made of PDMS with a base to curing agent ratio of 5:1, which simulates the softness of tissues. Lubricant oil is added between the PDMS layers to reduce the friction. The Kresling cells' high structural stiffness in the lateral direction helps the robot overcome the lateral resistance from the environment and separate the PDMS layers while moving forward.

The magnetic field profile used is shown in Figure 19. In this demonstration, a reversed magnetic field is applied at the end of the cycle to further help the Kresling cells expand against the

environmental resistance. The negative field strength indicates that the magnetic field acts in the opposite direction as $\mathbf{M}_{net}$.

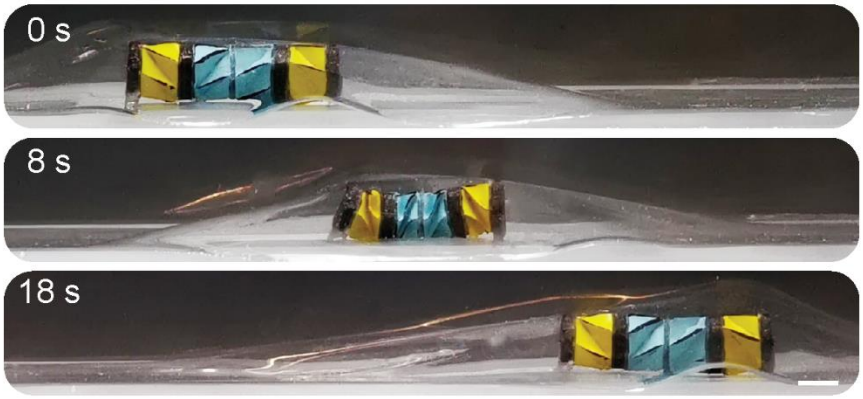

Figure 18: Robot crawling between two PDMS layers

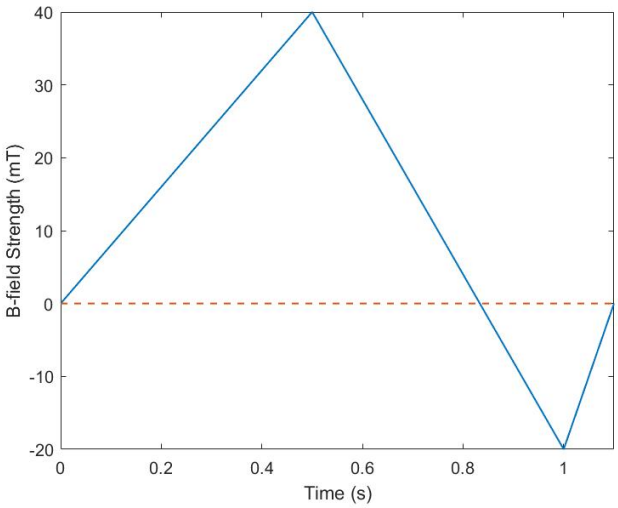

Figure 19: Magnetic field profile (1 cycle) for crawling in confined space

Drug Release Demonstration

Drug release within a confined space was simulated by loading the crawling robot with a pill and letting it dissolve in water. The pill is fabricated from a concentrated gel-based dye (Wilton

Brands LLC, USA) which is wrapped inside of a water-soluble paper (SmartSolve Industries, USA). This is inserted into the robot through the hole in the magnetic disk and Kresling unit cell, after which it is secured in place with Sil-Poxy adhesive. The robot is placed in an acrylic tank and distilled water is poured into the tank, dissolving the pill and releasing the dye as shown in Figure 20.

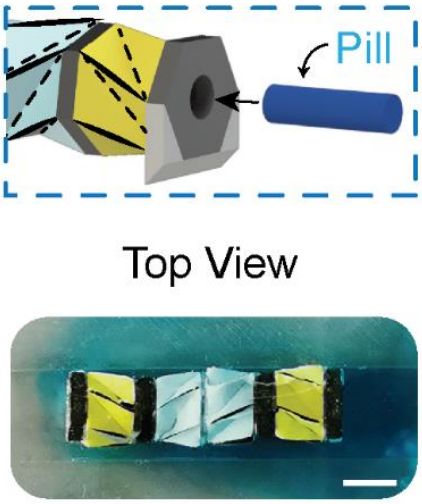

Figure 20: Pill inserted into through-hole of Kresling cell (above), dissolved dye in water (below)

Conclusion & Future work

In this study, a Kresling origami-based, magnetically actuated crawling robot was developed for the purpose of minimally invasive drug delivery. The Kresling origami inherently has an internal storage space ideal for storing drugs, and its anisotropic stiffness allows the robot to move even while overcoming the resistance from confined space. Magnetic actuation allows the Kresling cells to expand and fold quickly all while being untethered. The demonstrations show the crawling robot controlled freely in the *XY* plane.

The current crawling Kresling robot design is optimized for motion on flat surfaces. To be used for medical applications, it must be further tested and optimized for motion on living tissues with uneven terrains. Animal testing will eventually become necessary to confirm its effectiveness in navigating *in vivo*. Though the Kresling robot in this study is relatively small, further work can be done to downscale it more. This can further minimize the invasiveness of the robot on the human body. Additionally, sensors and actuators can be installed on the robot to allow more complex tasks within the body.

Acknowledgements

I give my sincere gratitude to the members of the Soft Intelligent Materials Laboratory for supporting me throughout this research: Dr. Zhao, Qiji Ze, Shuai Wu, Yue Sun, and Jize Dai. I would also like to acknowledge Dr. Glaucio Paulino and Larissa Novelino of the Georgia Institute of Technology who collaborated with us on this project. Lastly, I would like to thank Dr. Jonathan Song for being part of my thesis defense committee.

References

[1] JL Silverberg, et al., Using origami design principles to fold reprogrammable mechanical metamaterials. Science 345, 647–650 (2014).

[2] T Chen, OR Bilal, R Lang, C Daraio, K Shea, Autonomous deployment of a solar panel using elastic origami and distributed shape-memory-polymer actuators. Phys. Rev. Appl. 11, 064069 (2019).

[3] S Li, DM Vogt, D Rus, RJ Wood, Fluid-driven origami-inspired artificial muscles. Proc. Natl. academy Sci. 114, 13132–13137 (2017).

[4] Gultepe et al., Biopsy with thermally-responsive untethered microtools. Advanced Materials 25, 514-519 (2013)

[5] AM Bellinger et. al., Oral, ultra-long-lasting drug delivery: application toward malaria elimination goals. Science Translational Medicine 8 (2016).

[6] M. Boyvat, J.-S. Koh, R. J. Wood, Addressable wireless actuation for multijoint folding robots and devices. 5 Science Robotics 2, (2017).

[7] Kidambi, Wang, Dynamics of Kresling Origai Deployment. PhysRevE. 10.1103 (2020).

[8] L Novelino et al., Untethered control of functional origami microrobots with distributed actuation. PNAS (2020).